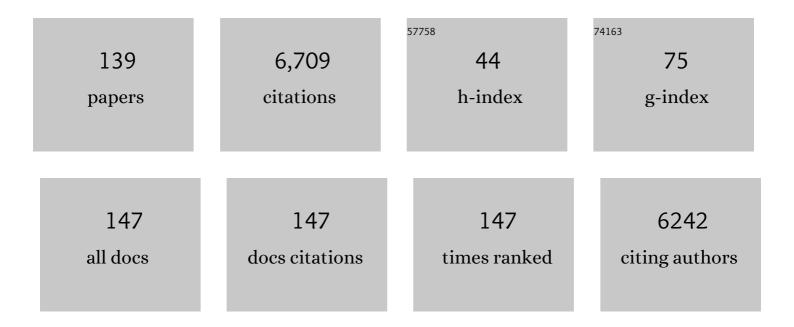
## Markus Nilsson

List of Publications by Year in descending order

Source: https://exaly.com/author-pdf/3899423/publications.pdf Version: 2024-02-01



#	Article	IF	CITATIONS
1	Induction of basal cell carcinomas and trichoepitheliomas in mice overexpressing GLI-1. Proceedings of the National Academy of Sciences of the United States of America, 2000, 97, 3438-3443.	7.1	352
2	A randomized clinical trial of neoadjuvant chemotherapy versus neoadjuvant chemoradiotherapy for cancer of the oesophagus or gastro-oesophageal junction. Annals of Oncology, 2016, 27, 660-667.	1.2	300
3	Imaging brain microstructure with diffusion MRI: practicality and applications. NMR in Biomedicine, 2019, 32, e3841.	2.8	266
4	Lifestyle related risk factors in the aetiology of gastro-oesophageal reflux. Gut, 2004, 53, 1730-1735.	12.1	258
5	Q-space trajectory imaging for multidimensional diffusion MRI of the human brain. NeuroImage, 2016, 135, 345-362.	4.2	256
6	Quantification of microscopic diffusion anisotropy disentangles effects of orientation dispersion from microstructure: Applications in healthy volunteers and in brain tumors. Neurolmage, 2015, 104, 241-252.	4.2	216
7	Neurite density imaging versus imaging of microscopic anisotropy in diffusion MRI: A model comparison using spherical tensor encoding. NeuroImage, 2017, 147, 517-531.	4.2	177
8	Microanisotropy imaging: quantification of microscopic diffusion anisotropy and orientational order parameter by diffusion MRI with magic-angle spinning of the q-vector. Frontiers in Physics, 2014, 2, .	2.1	163
9	Conventions and nomenclature for double diffusion encoding NMR and MRI. Magnetic Resonance in Medicine, 2016, 75, 82-87.	3.0	154
10	The importance of axonal undulation in diffusion MR measurements: a Monte Carlo simulation study. NMR in Biomedicine, 2012, 25, 795-805.	2.8	142
11	Noninvasive mapping of water diffusional exchange in the human brain using filterâ€exchange imaging. Magnetic Resonance in Medicine, 2013, 69, 1572-1580.	3.0	142
12	The link between diffusion MRI and tumor heterogeneity: Mapping cell eccentricity and density by diffusional variance decomposition (DIVIDE). NeuroImage, 2016, 142, 522-532.	4.2	141
13	Body Mass and Reflux Oesophagitis: an Oestrogen-dependent Association?. Scandinavian Journal of Gastroenterology, 2002, 37, 626-630.	1.5	134
14	The role of tissue microstructure and water exchange in biophysical modelling of diffusion in white matter. Magnetic Resonance Materials in Physics, Biology, and Medicine, 2013, 26, 345-370.	2.0	123
15	Resolution limit of cylinder diameter estimation by diffusion MRI: The impact of gradient waveform and orientation dispersion. NMR in Biomedicine, 2017, 30, e3711.	2.8	116
16	Constrained optimization of gradient waveforms for generalized diffusion encoding. Journal of Magnetic Resonance, 2015, 261, 157-168.	2.1	106
17	Searching for the neurite density with diffusion MRI: Challenges for biophysical modeling. Human Brain Mapping, 2019, 40, 2529-2545.	3.6	103
18	Apparent exchange rate mapping with diffusion MRI. Magnetic Resonance in Medicine, 2011, 66, 356-365.	3.0	102

#	Article	IF	CITATIONS
19	Neoadjuvant chemotherapy versus neoadjuvant chemoradiotherapy for cancer of the esophagus or gastroesophageal junction: long-term results of a randomized clinical trial. Ecological Management and Restoration, 2019, 32, .	0.4	101
20	Prevalence of gastro-oesophageal reflux symptoms and the influence of age and sex. Scandinavian Journal of Gastroenterology, 2004, 39, 1040-1045.	1.5	100
21	Biodegradation and biocompatability of a calcium sulphate-hydroxyapatite bone substitute. Journal of Bone and Joint Surgery: British Volume, 2004, 86-B, 120-125.	3.4	95
22	Filter-exchange PGSE NMR determination of cell membrane permeability. Journal of Magnetic Resonance, 2009, 200, 291-295.	2.1	93
23	On the effects of a varied diffusion time in vivo: is the diffusion in white matter restricted?. Magnetic Resonance Imaging, 2009, 27, 176-187.	1.8	88
24	Morbidity and mortality after surgery for cancer of the oesophagus and gastro-oesophageal junction: A randomized clinical trial of neoadjuvant chemotherapy vs. neoadjuvant chemoradiation. European Journal of Surgical Oncology, 2015, 41, 920-926.	1.0	86
25	Maxwellâ€compensated design of asymmetric gradient waveforms for tensorâ€valued diffusion encoding. Magnetic Resonance in Medicine, 2019, 82, 1424-1437.	3.0	81
26	Extrapolation-Based References Improve Motion and Eddy-Current Correction of High B-Value DWI Data: Application in Parkinson's Disease Dementia. PLoS ONE, 2015, 10, e0141825.	2.5	75
27	Quantification of microcirculatory parameters by joint analysis of flowâ€compensated and nonâ€flowâ€compensated intravoxel incoherent motion (IVIM) data. NMR in Biomedicine, 2016, 29, 640-649.	2.8	72
28	Regional values of diffusional kurtosis estimates in the healthy brain. Journal of Magnetic Resonance Imaging, 2013, 37, 610-618.	3.4	71
29	NMR diffusion-encoding with axial symmetry and variable anisotropy: Distinguishing between prolate and oblate microscopic diffusion tensors with unknown orientation distribution. Journal of Chemical Physics, 2015, 142, 104201.	3.0	70
30	Pharmacokinetics of gentamicin eluted from a regenerating bone graft substitute. Bone and Joint Research, 2016, 5, 427-435.	3.6	67
31	Optimal experimental design for filter exchange imaging: Apparent exchange rate measurements in the healthy brain and in intracranial tumors. Magnetic Resonance in Medicine, 2017, 77, 1104-1114.	3.0	67
32	Tensor-valued diffusion encoding for diffusional variance decomposition (DIVIDE): Technical feasibility in clinical MRI systems. PLoS ONE, 2019, 14, e0214238.	2.5	67
33	Towards unconstrained compartment modeling in white matter using diffusionâ€relaxation MRI with tensorâ€valued diffusion encoding. Magnetic Resonance in Medicine, 2020, 84, 1605-1623.	3.0	67
34	The dot-compartment revealed? Diffusion MRI with ultra-strong gradients and spherical tensor encoding in the living human brain. NeuroImage, 2020, 210, 116534.	4.2	64
35	Thermodynamic and Kinetic Characterization of Hostâ~Guest Association between Bolaform Surfactants and α- and β-Cyclodextrins. Journal of Physical Chemistry B, 2008, 112, 11310-11316.	2.6	63
36	Glioma Grade Discrimination with MR Diffusion Kurtosis Imaging: A Meta-Analysis of Diagnostic Accuracy. Radiology, 2018, 287, 119-127.	7.3	63

#	Article	IF	CITATIONS
37	Variability in diffusion kurtosis imaging: Impact on study design, statistical power and interpretation. NeuroImage, 2013, 76, 145-154.	4.2	62
38	Imaging brain tumour microstructure. NeuroImage, 2018, 182, 232-250.	4.2	62
39	Feeling old: being in a phase of transition in later life. Nursing Inquiry, 2000, 7, 41-49.	2.1	59
40	Early detection of macular changes in patients with diabetes using Rarebit Fovea Test and optical coherence tomography. British Journal of Ophthalmology, 2007, 91, 1596-1598.	3.9	59
41	Multidimensional diffusion MRI with spectrally modulated gradients reveals unprecedented microstructural detail. Scientific Reports, 2019, 9, 9026.	3.3	58
42	Tensorâ€valued diffusion MRI in under 3 minutes: an initial survey of microscopic anisotropy and tissue heterogeneity in intracranial tumors. Magnetic Resonance in Medicine, 2020, 83, 608-620.	3.0	55
43	Disentangling white-matter damage from physiological fibre orientation dispersion in multiple sclerosis. Brain Communications, 2020, 2, fcaa077.	3.3	55
44	Measurement Tensors in Diffusion MRI: Generalizing the Concept of Diffusion Encoding. Lecture Notes in Computer Science, 2014, 17, 209-216.	1.3	55
45	Interactions between Gemini Surfactants, 12-s-12, and $\hat{l}^2$ -cyclodextrin As Investigated by NMR Diffusometry and Electric Conductometry. Langmuir, 2006, 22, 8663-8669.	3.5	53
46	Evaluating the accuracy and precision of a two-compartment KÃ <b>¤</b> ger model using Monte Carlo simulations. Journal of Magnetic Resonance, 2010, 206, 59-67.	2.1	51
47	Diagnostic value ofÂalternative techniques to gadolinium-based contrast agents in MR neuroimaging—a comprehensive overview. Insights Into Imaging, 2019, 10, 84.	3.4	44
48	Gradient waveform design for tensor-valued encoding in diffusion MRI. Journal of Neuroscience Methods, 2021, 348, 109007.	2.5	44
49	Diffusion Tensor Tractography versus Volumetric Imaging in the Diagnosis of Behavioral Variant Frontotemporal Dementia. PLoS ONE, 2013, 8, e66932.	2.5	44
50	In vivo visualization of displacement-distribution-derived parameters in q-space imaging. Magnetic Resonance Imaging, 2008, 26, 77-87.	1.8	43
51	Systematic review and meta-analysis on the significance of salvage esophagectomy for persistent or recurrent esophageal squamous cell carcinoma after definitive chemoradiotherapy. Ecological Management and Restoration, 2016, 29, 734-739.	0.4	42
52	Accuracy of \$q\$-Space Related Parameters in MRI: Simulations and Phantom Measurements. IEEE Transactions on Medical Imaging, 2007, 26, 1437-1447.	8.9	39
53	Diffusionâ€weighted MRI measurements on stroke patients reveal waterâ€exchange mechanisms in subâ€acute ischaemic lesions. NMR in Biomedicine, 2009, 22, 619-628.	2.8	38
54	Disease-specific structural changes in thalamus and dentatorubrothalamic tract in progressive supranuclear palsy. Neuroradiology, 2015, 57, 1079-1091.	2.2	37

#	Article	IF	CITATIONS
55	Diffusion kurtosis imaging of gliomas grades II and III - a study of perilesional tumor infiltration, tumor grades and subtypes at clinical presentation. Radiology and Oncology, 2017, 51, 121-129.	1.7	37
56	Apparent exchange rate for breast cancer characterization. NMR in Biomedicine, 2016, 29, 631-639.	2.8	36
57	Alterations of Diffusion Kurtosis and Neurite Density Measures in Deep Grey Matter and White Matter in Parkinson's Disease. PLoS ONE, 2016, 11, e0157755.	2.5	35
58	Effects of restricted diffusion in a biological phantom: a q-space diffusion MRI study of asparagus stems at a 3T clinical scanner. Magnetic Resonance Materials in Physics, Biology, and Medicine, 2007, 20, 213-222.	2.0	34
59	Can restingâ€state functional MRI serve as a complement to taskâ€based mapping of sensorimotor function? A test–retest reliability study in healthy volunteers. Journal of Magnetic Resonance Imaging, 2011, 34, 511-517.	3.4	34
60	Blood and cerebrospinal fluid neurofilament light differentially detect neurodegeneration in early Alzheimer's disease. Neurobiology of Aging, 2020, 95, 143-153.	3.1	34
61	Survival benefit and additional value of preoperative chemoradiotherapy in resectable gastric and gastro-oesophageal junction cancer: A direct and adjusted indirect comparison meta-analysis. European Journal of Surgical Oncology, 2015, 41, 282-294.	1.0	33
62	Diffusion MRI microstructure models with in vivo human brain Connectome data: results from a multiâ€group comparison. NMR in Biomedicine, 2017, 30, e3734.	2.8	33
63	The effect of white matter hyperintensities on statistical analysis of diffusion tensor imaging in cognitively healthy elderly and prodromal Alzheimer's disease. PLoS ONE, 2017, 12, e0185239.	2.5	32
64	Timeâ€dependent diffusion in undulating thin fibers: Impact on axon diameter estimation. NMR in Biomedicine, 2020, 33, e4187.	2.8	31
65	Biodegradation and biocompatability of a calcium sulphate-hydroxyapatite bone substitute. Journal of Bone and Joint Surgery: British Volume, 2004, 86, 120-5.	3.4	31
66	Assessment of Global and Regional Diffusion Changes along White Matter Tracts in Parkinsonian Disorders by MR Tractography. PLoS ONE, 2013, 8, e66022.	2.5	29
67	Altered white matter microstructure in lupus patients: a diffusion tensor imaging study. Arthritis Research and Therapy, 2018, 20, 21.	3.5	28
68	Tensorâ€valued diffusion MRI differentiates cortex and white matter in malformations of cortical development associated with epilepsy. Epilepsia, 2020, 61, 1701-1713.	5.1	28
69	Outcome of neoadjuvant therapies for cancer of the oesophagus or gastro-oesophageal junction based on a national data registry. British Journal of Surgery, 2016, 103, 1864-1873.	0.3	26
70	Cumulant expansions for measuring water exchange using diffusion MRI. Journal of Chemical Physics, 2018, 148, 074109.	3.0	26
71	Intravoxel incoherent motion (IVIM) imaging at different magnetic field strengths: What is feasible?. Magnetic Resonance Imaging, 2014, 32, 1247-1258.	1.8	23
72	Alteration of putaminal fractional anisotropy in Parkinson's disease: a longitudinal diffusion kurtosis imaging study. Neuroradiology, 2018, 60, 247-254.	2.2	23

#	Article	IF	CITATIONS
73	Diffusion tensor imaging and tractography of the white matter in normal aging: The rate-of-change differs between segments within tracts. Magnetic Resonance Imaging, 2018, 45, 113-119.	1.8	22
74	Subjectively Reported Effects Experienced in an Actively Shielded 7T MRI: A Large cale Study. Journal of Magnetic Resonance Imaging, 2020, 52, 1265-1276.	3.4	21
75	Regional structural hypo―and hyperconnectivity of frontal–striatal and frontal–thalamic pathways in behavioral variant frontotemporal dementia. Human Brain Mapping, 2018, 39, 4083-4093.	3.6	21
76	Diffusion Tensor MRI to Distinguish Progressive Supranuclear Palsy from α-Synucleinopathies. Radiology, 2019, 293, 646-653.	7.3	20
77	Motionâ€compensated bâ€tensor encoding for in vivo cardiac diffusionâ€weighted imaging. NMR in Biomedicine, 2020, 33, e4213.	2.8	20
78	Neural networks for parameter estimation in microstructural MRI: Application to a diffusion-relaxation model of white matter. NeuroImage, 2021, 244, 118601.	4.2	20
79	Dimensionality reduction of fMRI time series data using locally linear embedding. Magnetic Resonance Materials in Physics, Biology, and Medicine, 2010, 23, 327-338.	2.0	19
80	Multicomponent Interdiffusion and Self-Diffusion of the Cationic Poly{[9,9-bis(6′- <i>N</i> , <i>N</i> , <i>N</i> , trimethylammonium)hexyl]fluorene-phenylene} Dibromide in a Dimethyl Sulfoxide + Water Solution. Journal of Chemical & Engineering Data, 2010, 55, 1860-1866.	1.9	18
81	Spatial analysis of diffusion tensor tractography statistics along the inferior fronto-occipital fasciculus with application in progressive supranuclear palsy. Magnetic Resonance Materials in Physics, Biology, and Medicine, 2013, 26, 527-537.	2.0	18
82	Liquid crystal phantom for validation of microscopic diffusion anisotropy measurements on clinical MRI systems. Magnetic Resonance in Medicine, 2018, 79, 1817-1828.	3.0	18
83	The Käger vs bi-exponential model: Theoretical insights and experimental validations. Journal of Magnetic Resonance, 2018, 296, 72-78.	2.1	18
84	Mapping of apparent susceptibility yields promising diagnostic separation of progressive supranuclear palsy from other causes of parkinsonism. Scientific Reports, 2019, 9, 6079.	3.3	18
85	Monte Carlo Simulations of Water Exchange Through Myelin Wraps: Implications for Diffusion MRI. IEEE Transactions on Medical Imaging, 2019, 38, 1438-1445.	8.9	17
86	Improved fibre dispersion estimation using b-tensor encoding. NeuroImage, 2020, 215, 116832.	4.2	17
87	Association between time interval from neoadjuvant chemoradiotherapy to surgery and complete histological tumor response in esophageal and gastroesophageal junction cancer: a national cohort study. Ecological Management and Restoration, 2020, 33, .	0.4	16
88	Adjuvant radiotherapy for gastric cancer—end of the road?. Annals of Oncology, 2021, 32, 287-289.	1.2	16
89	SPHERIOUSLY? The challenges of estimating sphere radius non-invasively in the human brain from diffusion MRI. NeuroImage, 2021, 237, 118183.	4.2	16
90	Reproducibility of psychophysics and electroencephalography during offset analgesia. European Journal of Pain, 2014, 18, 824-834.	2.8	15

#	Article	IF	CITATIONS
91	Grey and White Matter Clinico-Anatomical Correlates of Disinhibition in Neurodegenerative Disease. PLoS ONE, 2016, 11, e0164122.	2.5	15
92	Effects of APOE ε4 on neuroimaging, cerebrospinal fluid biomarkers, and cognition in prodromal Alzheimer's disease. Neurobiology of Aging, 2018, 71, 81-90.	3.1	15
93	Vancomycin elution from a biphasic ceramic bone substitute. Bone and Joint Research, 2019, 8, 49-54.	3.6	15
94	Perception of very small visual stimuli in the fovea: normative data for the Rarebit Foveal Test. Australasian journal of optometry, The, 2006, 89, 81-85.	1.3	14
95	Time dependence in diffusion MRI predicts tissue outcome in ischemic stroke patients. Magnetic Resonance in Medicine, 2021, 86, 754-764.	3.0	14
96	Single center consecutive series cohort study of minimally invasive versus open resection for cancer in the esophagus or gastroesophageal junction. Ecological Management and Restoration, 2018, 31, .	0.4	13
97	Microstructural white matter alterations associated to neurocognitive deficits in childhood leukemia survivors treated with cranial radiotherapy – a diffusional kurtosis study. Acta Oncológica, 2019, 58, 1021-1028.	1.8	13
98	Brain Tumor Characterization Using Multibiometric Evaluation of MRI. Tomography, 2018, 4, 14-25.	1.8	12
99	Mapping prostatic microscopic anisotropy using linear and spherical bâ€ŧensor encoding: A preliminary study. Magnetic Resonance in Medicine, 2021, 86, 2025-2033.	3.0	12
100	Shortâ€ŧerm effects experienced during examinations in an actively shielded 7 T MR. Bioelectromagnetics, 2019, 40, 234-249.	1.6	11
101	Texture analysis of computed tomography data using morphologic and metabolic delineation of esophageal cancer—relation to tumor type and neoadjuvant therapy response. Ecological Management and Restoration, 2019, 32, .	0.4	11
102	Accuracy and precision in super-resolution MRI: Enabling spherical tensor diffusion encoding at ultra-high b-values and high resolution. NeuroImage, 2021, 245, 118673.	4.2	11
103	Histogram analysis of tensor-valued diffusion MRI in meningiomas: Relation to consistency, histological grade and type. NeuroImage: Clinical, 2022, 33, 102912.	2.7	11
104	On the generalizability of diffusion MRI signal representations across acquisition parameters, sequences and tissue types: Chronicles of the MEMENTO challenge. NeuroImage, 2021, 240, 118367.	4.2	10
105	Magic DIAMOND: Multi-fascicle diffusion compartment imaging with tensor distribution modeling and tensor-valued diffusion encoding. Medical Image Analysis, 2021, 70, 101988.	11.6	9
106	Comparison of Macular Thickness in Patients with Keratoconus and Control Subjects Using the Cirrus HD-OCT. BioMed Research International, 2015, 2015, 1-5.	1.9	8
107	Vertical imbalance induced by prism-ballasted soft toric contact lenses fitted unilaterally. Ophthalmic and Physiological Optics, 2008, 28, 157-162.	2.0	7
108	Cortical and white matter correlates of languageâ€learning aptitudes. Human Brain Mapping, 2021, 42, 5037-5050.	3.6	7

#	Article	IF	CITATIONS
109	Preoperative Quantitative MR Tractography Compared with Visual Tract Evaluation in Patients with Neuropathologically Confirmed Gliomas Grades II and III: A Prospective Cohort Study. Radiology Research and Practice, 2016, 2016, 1-15.	1.3	6
110	Probing tissue microstructure by diffusion skewness tensor imaging. Scientific Reports, 2021, 11, 135.	3.3	6
111	Post-Concussive Vestibular Dysfunction Is Related to Injury to the Inferior Vestibular Nerve. Journal of Neurotrauma, 2022, 39, 829-840.	3.4	6
112	Clinical importance of spherical and chromatic aberration on the accommodative response in contact lens wear. Journal of Modern Optics, 2011, 58, 1696-1702.	1.3	5
113	Cortical thickness of Broca's area and right homologue is related to grammar learning aptitude and pitch discrimination proficiency. Brain and Language, 2019, 188, 42-47.	1.6	5
114	Mortality after surgery for primary hyperparathyroidism: results from a nationwide cohort. British Journal of Surgery, 2021, 108, 858-863.	0.3	5
115	Sensitivity of Diffusion MRI to White Matter Pathology: Influence of Diffusion Protocol, Magnetic Field Strength, and Processing Pipeline in Systemic Lupus Erythematosus. Frontiers in Neurology, 2022, 13, 837385.	2.4	5
116	Evaluation of small-volume tubes for venous and capillary PT (INR) samples. International Journal of Laboratory Hematology, 2015, 37, 699-704.	1.3	4
117	Normal radiological lymph node appearance in the thorax. Ecological Management and Restoration, 2019, 32, 1-6.	0.4	4
118	Assessment of spatial BOLD sensitivity variations in fMRI using gradient-echo field maps. Magnetic Resonance Imaging, 2010, 28, 947-956.	1.8	3
119	Evaluation of the anterior chamber angle in keratoconus and normal subjects. Contact Lens and Anterior Eye, 2015, 38, 277-282.	1.7	3
120	Stay on the Beat With Tensor-Valued Encoding: Time-Dependent Diffusion and Cell Size Estimation in ex vivo Heart. Frontiers in Physics, 2022, 10, .	2.1	3
121	Optimal experimental design for filter exchange imaging: Apparent exchange rate measurements in the healthy brain and in intracranial tumors. Magnetic Resonance in Medicine, 2017, 77, C1-C1.	3.0	2
122	Diffusion tensor imaging in glioblastoma patients treated with volumetric modulated arc radiotherapy: a longitudinal study. Acta OncolÃ <sup>3</sup> gica, 2022, 61, 680-687.	1.8	2
123	Molecular Exchange between Intra- and Extracellular Compartments in a Cell Suspension. , 2008, , .		1
124	Scintillate: An open-source graphical viewer for time-series calcium imaging evaluation and pre-processing. Journal of Neuroscience Methods, 2016, 273, 120-127.	2.5	1
125	Assessing Tissue Heterogeneity by non-Gaussian Measures in a Permeable Environment. , 2018, , .		1
126	Foveal function in children treated for amblyopia. Acta Ophthalmologica, 0, 85, 0-0.	0.3	1

8

#	Article	IF	CITATIONS
127	Solid phase ELISA for serum ferritin. Scandinavian Journal of Clinical and Laboratory Investigation, 1980, 40, 641-645.	1.2	1
128	O148 SHORT-TERM RESULTS OF A RANDOMIZED CONTROLLED TRIAL OF STANDARD VS. PROLONGED TIME TO SURGERY AFTER NEOADJUVANT CHEMORADIATION FOR CANCER. Ecological Management and Restoration, 2019, 32, .	0.4	0
129	Experiences of specialist social workers for asylum seeking patients at a large Swedish hospital. European Journal of Public Health, 2019, 29, .	0.3	0
130	Characteristics of specialist consultations regarding immigrant patients at a large Swedish hospital. European Journal of Public Health, 2019, 29, .	0.3	0
131	Reply to letter: Neoadjuvant chemoradiotherapy or chemotherapy for esophageal cancer: what is the current evidence?. Ecological Management and Restoration, 2019, 32, .	0.4	0
132	Macular abnormalities and the Rarebit Fovea Test. Acta Ophthalmologica, 0, 85, 0-0.	0.3	0
133	Improved analysis of the outer foveal microstructure - OCT imaging of healthy and abnormal retina. Acta Ophthalmologica, 2014, 92, 0-0.	1.1	0
134	Objective assessment of cataract: Comparison between the Lens Opacities Classification System III and a Scheimpflug camera. Acta Ophthalmologica, 2015, 93, n/a-n/a.	1.1	0
135	Use of directional optical coherence tomography and selected landmarks to determine foveal topography and microstructure. A strategy to characterize differences between normal and expremature cases. Acta Ophthalmologica, 2015, 93, n/a-n/a.	1.1	0
136	Reduced retinal nerve fibre layer thickness in multiple sclerosis patients with and without history of optic neuritis. Acta Ophthalmologica, 2015, 93, n/a-n/a.	1.1	0
137	Umfangreiche epidemiologische und Genotyp-PhÃ <b>¤</b> otyp (GxP) Analysen in dem weltweit größten Patientenkollektiv mit idiopathischer Achalasie. Zeitschrift Fur Gastroenterologie, 2017, 55, .	0.5	0
138	Separating Glioma Hyperintensities From White Matter by Diffusion-Weighted Imaging With Spherical Tensor Encoding. Frontiers in Neuroscience, 2022, 16, 842242.	2.8	0
139	205: ADJUNCTIVE SURVEILLANCE MODALITIES AND ONCOLOGIC OUTCOME: A REPORT FROM THE ENSURE STUDY. Ecological Management and Restoration, 2022, 35, .	0.4	0